Exact gravity dual of a gapless superconductor

JHEP07(2009)026

(http://iopscience.iop.org/1126-6708/2009/07/026)

Published by IOP Publishing for SISSA

Received: *February 19, 2009*
Revised: *June 16, 2009*
Accepted: *June 17, 2009*
Published: *July 9, 2009*

JHEP07(2009)026

Exact gravity dual of a gapless superconductor

George Koutsoumbas,[a] **Eleftherios Papantonopoulos**[a] **and George Siopsis**[b]

[a] *Department of Physics, National Technical University of Athens, Zografou Campus GR 157 73, Athens, Greece*

[b] *Department of Physics and Astronomy, The University of Tennessee, Knoxville, TN 37996 - 1200, U.S.A.*

E-mail: kutsubas@central.ntua.gr, lpapa@central.ntua.gr, siopsis@tennessee.edu

Abstract: A model of an exact gravity dual of a gapless superconductor is presented in which the condensate is provided by a charged scalar field coupled to a bulk black hole of hyperbolic horizon in asymptotically AdS spacetime. A critical temperature exists at which the mass of the black hole vanishes and a scaling symmetry emerges. Below the critical point, the black hole acquires its hair through a phase transition while an electromagnetic perturbation of the background Maxwell field determines the conductivity of the boundary theory.

Keywords: AdS-CFT Correspondence, Black Holes

ArXiv ePrint: 0902.0733

doi:10.1088/1126-6708/2009/07/026

Contents

JHEP07(2009)026

1 Introduction

The AdS/CFT correspondence has become a powerful tool in studying strongly coupled phenomena in quantum field theory using results from a weakly coupled gravity background. According to this correspondence principle [1], a string theory on asymptotically AdS spacetimes can be related to a conformal field theory on the boundary. In recent years, apart from string theory, this holographic correspondence, following a more phenomenological approach, has also been applied to nuclear physics in order to describe certain aspects such as heavy ion collisions at RHIC [2] and to certain condensed matter systems. Phenomena such as the Hall effect [3] and Nernst effect [4–6] have dual gravitational descriptions.

Recently the AdS/CFT correspondence has also been applied to superconductivity [7]. The gravity dual of a superconductor consists of a system with a black hole and a charged scalar field, in which the black hole admits scalar hair at temperature smaller than a critical temperature, while there is no scalar hair at larger temperatures. A condensate of the charged scalar field is formed through its coupling to a Maxwell field of the background. Neither field was backreacting on the metric. This decoupled Abelian-Higgs sector can be obtained from an Einstein-Maxwell-scalar theory [8] through a scaling limit in which the product of the charge of the black hole and the charge of the scalar field is held fixed while the latter is taken to infinity. Considering fluctuations of the vector potential, the frequency dependent conductivity was calculated, and it was shown that it develops a gap determined by the condensate.

The model of the gravitational dual to the superconductor in [7] was further studied beyond the probe limit [9]. Away from the large charge limit, the backreaction of the scalar field to the spacetime metric has to be taken into consideration. It was found

that all the essential characteristics of the dual superconductor were persisting. Moreover, even for very small charge the superconductivity was maintained. These models however are phenomenological models. The classical fields and their interactions are chosen by hand. It would have also been desirable that these models emerge from a consistent string theory [10].

In this work we propose a model of a gravity dual of a gapless superconductor in which a charged scalar field provides the scalar hair of an exact black hole solution [11, 12]. It has been shown in [13] that, below a critical temperature, this black hole solution undergoes a spontaneous dressing up with the scalar hair, while above that critical temperature the dressed black hole decays into the bare black hole. At the critical point, the mass of the black hole vanishes and a scaling symmetry emerges, because the metric becomes purely AdS. We will show that, if the scalar field coupled to gravity in the bulk is charged, a condensate forms, while an electromagnetic perturbation of the background determines the conductivity and therefore the superfluid density of the boundary theory. There is evidence that these black hole solutions can be obtained from eleven-dimensional supergravity theory [14].

The paper is organized as follows. In section 2 we discuss an exact black hole solution with scalar hair and in section 3 we explain how the black hole acquires its hair through a third order phase transition. In section 4 we outline a stability analysis of hairy black holes. In section 5 we discuss the dual superconductor on the boundary of the exact hairy black hole solution and calculate its conductivity and superfluid density analytically. In section 6 we support our analytical results of section 5 with a numerical investigation and present evidence showing that the superconductor is gapless. Finally, section 7 contains our concluding remarks.

2 Black hole with scalar hair

To obtain a black hole with scalar hair, we start with the four-dimensional action

$$I = I_{gr} + I_{\text{matter}} \tag{2.1}$$

consisting of the Einstein-Hilbert action with a negative cosmological constant $\Lambda = -\frac{3}{l^2}$,

$$I_{gr} = \frac{1}{16\pi G}\int d^4x\sqrt{-g}\left[R + \frac{6}{l^2}\right] \tag{2.2}$$

where G is Newton's constant, R is the Ricci scalar, l is the AdS radius and a charged scalar together with a Maxwell field (matter fields)

$$I_{\text{matter}} = \int d^4x\sqrt{-g}\left[g^{\mu\nu}D_\mu\phi(D_\nu\phi)^* - \frac{1}{6}R\phi^*\phi - \lambda(\phi^*\phi)^2\right] - \frac{1}{4}\int d^4x\sqrt{-g}F^{\mu\nu}F_{\mu\nu}\,, \tag{2.3}$$

where

$$D_\mu\phi \equiv \partial_\mu\phi + iqA_\mu\phi \tag{2.4}$$

JHEP07(2009)026

and λ is an arbitrary coupling constant. The corresponding field equations are

$$\begin{aligned} G_{\mu\nu} - \frac{3}{l^2} g_{\mu\nu} &= 8\pi G T^{\text{matter}}_{\mu\nu} \,, \\ D_\mu D^\mu \phi &= \frac{1}{6} R\phi + \lambda \phi |\phi|^2 \,, \\ \frac{1}{\sqrt{-g}} \partial_\nu (\sqrt{-g} F^{\mu\nu}) &= J^\mu \,, \end{aligned} \tag{2.5}$$

where the energy-momentum tensor is given by

$$T^{\mu\nu}_{\text{matter}} = \frac{1}{\sqrt{-g}} \frac{\delta I_{\text{matter}}}{\delta g_{\mu\nu}} \,, \tag{2.6}$$

and the electric current is

$$J_\mu = iq(\phi^* D_\mu \phi - \text{c.c.}) \,. \tag{2.7}$$

The presence of a negative cosmological constant allows the existence of black holes with topology $\mathbb{R}^2 \times \Sigma$, where Σ is a two-dimensional manifold of constant negative curvature. These black holes are known as topological black holes (TBHs) [15, 16]. The simplest solution reads

$$ds^2 = -f_{TBH}(\rho) dt^2 + \frac{1}{f_{TBH}(\rho)} d\rho^2 + \rho^2 d\sigma^2 \quad , \quad f_{TBH}(\rho) = \frac{\rho^2}{l^2} - 1 - \frac{\rho_0}{\rho} \,, \tag{2.8}$$

with $\phi = 0$, $A_\mu = 0$. ρ_0 is a constant which is proportional to the mass and is bounded from below ($\rho_0 \geq -\frac{2}{3\sqrt{3}} l$). $d\sigma^2$ is the line element of the two-dimensional manifold Σ, which is locally isomorphic to the hyperbolic manifold H^2 and of the form

$$\Sigma = H^2/\Gamma \quad , \quad \Gamma \subset O(2,1) \,, \tag{2.9}$$

where Γ is a freely acting discrete subgroup (i.e., without fixed points) of isometries. The line element $d\sigma^2$ of Σ can be written as

$$d\sigma^2 = d\theta^2 + \sinh^2 \theta d\varphi^2 \,, \tag{2.10}$$

with $\theta \geq 0$ and $0 \leq \varphi < 2\pi$ being the coordinates of the hyperbolic space H^2 or pseudosphere, which is a non-compact two-dimensional space of constant negative curvature. This space becomes a compact space of constant negative curvature with genus $\text{g} \geq 2$ by identifying, according to the connection rules of the discrete subgroup Γ, the opposite edges of a 4g-sided polygon whose sides are geodesics and is centered at the origin $\theta = \varphi = 0$ of the pseudosphere [15–17]. An octagon is the simplest such polygon, yielding a compact surface of genus $\text{g} = 2$ under these identifications. Thus, the two-dimensional manifold Σ is a compact Riemann 2-surface of genus $\text{g} \geq 2$. The configuration (2.8) is an asymptotically locally AdS spacetime. The horizon structure of (2.8) is determined by the roots of the metric function $f_{TBH}(\rho)$, that is

$$f_{TBH}(\rho) = \frac{\rho^2}{l^2} - 1 - \frac{\rho_0}{\rho} = 0 \,. \tag{2.11}$$

JHEP07(2009)026

For $-\frac{2}{3\sqrt{3}}l < \rho_0 < 0$, this equation has two distinct non-degenerate solutions, corresponding to an inner and an outer horizon ρ_- and ρ_+ respectively. For $\rho_0 \geq 0$, $f_{TBH}(\rho)$ has just one non-degenerate root and so the black hole (2.8) has one horizon ρ_+. The horizons for both cases of ρ_0 have the non-trivial topology of the manifold Σ. We note that for $\rho_0 = -\frac{2}{3\sqrt{3}}l$, $f_{TBH}(\rho)$ has a degenerate root, but this horizon does not have an interpretation as black hole horizon [15].

The boundary has metric

$$ds^2_\partial = -dt^2 + l^2 d\sigma^2 \tag{2.12}$$

so spatially it is a hyperbolic manifold of radius l (and of curvature $-1/l$).

The temperature, entropy and mass of the black hole are, respectively,

$$T = \frac{3}{4\pi l}\left(\frac{\rho_+}{l} - \frac{l}{3\rho_+}\right), \quad S_{TBH} = \frac{\sigma\rho_+^2}{4G}, \quad M_{TBH} = \frac{\sigma\rho_+}{8\pi G}\left(\frac{\rho_+^2}{l^2} - 1\right). \tag{2.13}$$

obeying the law of thermodynamics $dM = TdS$.

A static black hole solution with topology $\mathbb{R}^2 \times \Sigma$ and scalar hair, is given by (MTZ black hole) [11]

$$ds^2 = -f_{MTZ}(r)dt^2 + \frac{dr^2}{f_{MTZ}(r)} + r^2 d\sigma^2 \quad , \quad f_{MTZ} = \frac{r^2}{l^2} - \left(1 + \frac{r_0}{r}\right)^2, \tag{2.14}$$

with

$$\phi(r) = \frac{1}{\sqrt{2}}\Psi(r) \ , \quad A_\mu = 0 \ . \tag{2.15}$$

where

$$\Psi(r) \equiv -\sqrt{\frac{3}{4\pi G}}\frac{r_0}{r + r_0} \tag{2.16}$$

is the form of the scalar hair found in the case of a *real* scalar field [11, 12]. Our normalization is slightly different due to the fact that we have a *complex* scalar field. Also, we have chosen a negative sign in (2.16) so that the condensates take on positive values.

The above hairy black hole solution is obtained for the special value of the coupling constant

$$\lambda = \frac{8\pi G}{3l^2} \ . \tag{2.17}$$

Other solutions (charged black holes) also exist for values of λ below the above critical value in the case of a *real* scalar field [12]. It would be interesting to extend those solutions to the case of a *complex* scalar field ϕ as well.

The conformally coupled scalar field $|\phi|$ can be turned into a minimally coupled field through the field redefinition

$$\hat{g}_{\mu\nu} = \left(1 - \frac{8\pi G}{3}|\phi|^2\right) g_{\mu\nu} \ , \quad \hat{\phi} = \sqrt{\frac{3}{8\pi G}}\tanh^{-1}\sqrt{\frac{8\pi G}{3}}|\phi| \ . \tag{2.18}$$

The action involving the real scalar field $\hat{\phi}$ is

$$I_{\hat{\phi}} = \int d^4x\sqrt{-\hat{g}}\left[\frac{1}{2}\hat{g}^{\mu\nu}\partial_\mu\hat{\phi}\partial_\nu\hat{\phi} - V(\hat{\phi}) + \dots\right] \tag{2.19}$$

JHEP07(2009)026

where

$$V(\hat{\phi}) = -\frac{3}{4\pi G l^2}\sinh^2\sqrt{\frac{4\pi G}{3}}\hat{\phi}\ . \tag{2.20}$$

and the dots represent interaction terms involving other fields, showing that the mass of the scalar field is $m^2 = -2/l^2$. This mass satisfies the Breitenlohner-Friedman (BF) bound ensuring the perturbative stability of AdS spacetime [18, 19]. However, the BF bound does not guarantee the nonlinear stability of hairy black holes under general boundary conditions and potentials. Therefore, a careful treatment of the stability issue is needed. In section 4 we give the main results of the stability analysis while more details can be found in [20].

The temperature, entropy and mass of the black hole are given respectively by [11]

$$T = \frac{1}{\pi}\left(\frac{r_+}{l} - \frac{1}{2}\right)\ , \quad S_{MTZ} = \frac{\sigma l^2}{4G}\left(2\frac{r_+}{l} - 1\right)\ , \quad M_{MTZ} = \frac{\sigma r_+}{4\pi G}\left(\frac{r_+}{l} - 1\right)\ . \tag{2.21}$$

It is easy to show that the law of thermodynamics $dM = TdS$ holds.

For non-negative mass, $M_{MTZ} \geq 0$, this black hole possesses only one event horizon at

$$r_+ = \frac{l}{2}\left(1 + \sqrt{1 + 4\frac{r_0}{l}}\right)\ , \tag{2.22}$$

and ϕ is regular everywhere. For negative masses, $-l/4 < r_0 < 0$, the metric (2.14) develops three horizons, two of which are event horizons located at r_{--} and at r_+

$$\begin{aligned} r_{--} &= \frac{l}{2}\left(-1 + \sqrt{1 - 4\frac{r_0}{l}}\right)\ , \\ r_- &= \frac{l}{2}\left(1 - \sqrt{1 + 4\frac{r_0}{l}}\right)\ , \\ r_+ &= \frac{l}{2}\left(1 + \sqrt{1 + 4\frac{r_0}{l}}\right)\ , \end{aligned} \tag{2.23}$$

which satisfy $0 < r_{--} < -r_0 < r_- < l/2 < r_+$. The scalar field ϕ is singular at $r = -r_0$.

Note that if $\rho_0 = 0$, $r_0 = 0$, then both the MTZ black hole (2.14) and the TBH black hole (2.8) go to

$$ds^2_{\rm AdS} = -\left[\frac{r^2}{l^2} - 1\right]dt^2 + \left[\frac{r^2}{l^2} - 1\right]^{-1}dr^2 + r^2 d\sigma^2\ , \tag{2.24}$$

which is a manifold of negative constant curvature possessing an event horizon at $r = l$. The MTZ and TBH black holes match continuously at the critical temperature

$$T_0 = \frac{1}{2\pi l} \tag{2.25}$$

which corresponds to $M_{TBH} = M_{MTZ} = 0$, with (2.24) being a transient configuration. Evidently, at the critical point (2.25) a scaling symmetry emerges owing to the fact that the metric becomes pure AdS.

3 Phase transition

In this section we will review the results discussed in [13] of a phase transition of a vacuum TBH to MTZ below the critical temperature (2.25).

Defining the free energy as $F = M - TS$ and using relations (2.21), we obtain

$$F_{MTZ} = -\frac{\sigma l}{8\pi G}\left(\frac{2r_+^2}{l^2} - \frac{2r_+}{l} + 1\right) . \tag{3.1}$$

The free energy (3.1) can be written in terms of the temperature as

$$F_{MTZ} = -\frac{\sigma l}{8\pi G}\Big(1 + 2\pi l(T - T_0) + 2\pi^2 l^2 (T - T_0)^2\Big) , \tag{3.2}$$

where $T_0 \approx 0.160/l$ is the critical temperature (2.25).

On the other hand, the free energy of the TBH, using relations (2.13), is

$$F_{TBH} = -\frac{\sigma \rho_+}{16\pi G}\left(\frac{\rho_+^2}{l^2} + 1\right) , \tag{3.3}$$

which can be expanded around the critical temperature T_0 as

$$F_{TBH} = -\frac{\sigma l}{8\pi G}\Big(1 + 2\pi l(T - T_0) + 2\pi^2 l^2 (T - T_0)^2 + \pi^3 l^3 (T - T_0)^3 + \dots\Big) . \tag{3.4}$$

Using (3.2) and (3.4), we can calculate the difference between the TBH and MTZ free energies. We obtain

$$\Delta F = F_{TBH} - F_{MTZ} = -\frac{\sigma l}{8\pi G}\, \pi^3 l^3 (T - T_0)^3 + \dots , \tag{3.5}$$

indicating a third order phase transition between MTZ and TBH at the critical temperature T_0. Matching the temperatures of the MTZ black hole and the TBH we obtain

$$\frac{r_+}{l} = \frac{3\rho_+}{4l} - \frac{l}{4\rho_+} + \frac{1}{2} . \tag{3.6}$$

It is easily seen that $r_+ \leq \rho_+$, and the inequality is saturated for $r_+ = \rho_+ = l$. We remark that the temperature T should be non-negative, so $r_+ \geq \frac{l}{2}$ for the MTZ black hole and $\rho_+ \geq \frac{l}{\sqrt{3}}$ for the TBH.

Thermodynamically we can understand this phase transition as follows. Using relations (2.21), (2.13) and (3.6), we find that $S_{TBH} > S_{MTZ}$ and $M_{TBH} > M_{MTZ}$ for the relevant ranges of the horizons r_+ or ρ_+. If $r_+ > l$ (i.e., the radius of the horizon exceeds the radius of the boundary and $T > T_0$), both black holes have positive mass. As $T > T_0$ implies $F_{TBH} \leq F_{MTZ}$, the MTZ black hole dressed with the scalar field will decay into the bare black hole. In the decay process, the scalar black hole absorbs energy from the thermal bath, increasing its horizon radius (from r_+ to $\rho_+ > r_+$) and consequently its entropy. Therefore, in a sense the scalar field is absorbed by the black hole.

If $r_+ < l$ (i.e., the radius of the boundary exceeds the radius of the horizon and $T < T_0$), both black holes have negative mass, but now $F_{TBH} > F_{MTZ}$, which means that

JHEP07(2009)026

the MTZ configuration with nonzero scalar field is favorable. As a consequence, below the critical temperature, the bare black hole undergoes a spontaneous "dressing up" with the scalar field. In the process, the mass and entropy of the black hole decrease and the differences in energy and entropy are transferred to the heat bath.

At the critical temperature, the thermodynamic functions of the two phases match continuously, hence the phase transition is not of first order. The order parameter that characterizes the transition can be defined in terms of the value of the scalar field at the horizon; using the solution for the scalar field (2.15) we obtain for $T < T_0$,

$$\lambda_\phi = \left| \tanh \sqrt{\frac{8\pi G}{3}} \phi(r_+) \right| = \left| \frac{r_+ - l}{r_+} \right| = \frac{T_0 - T}{T_0 + T} \quad . \tag{3.7}$$

For $T > T_0$, λ_ϕ vanishes. Therefore the order parameter $\lambda_\phi(T)$ is continuous at the critical temperature but its first derivative jumps from $-\frac{1}{2T_0}$ to 0 as we cross the critical point.

The pure AdS space of (2.24) has free energy $F_{AdS} = -\frac{\sigma l}{8\pi G}$ as can be easily seen using relations (3.1) or (3.3) with $r_+ = l$. Then observe that F_{AdS} is the constant term of both F_{MTZ} in (3.2) and F_{TBH} in (3.4). Hence the difference of free energies of TBH or MTZ black holes with the free energy of pure AdS space indicates that the configuration (2.24) is transient between the MTZ and TBH phase transition. At the critical point the mass of the black hole vanishes and a scaling symmetry emerges.

Further evidence of this phase transition was provided in [13]. The QNMs of the electromagnetic perturbations of the MTZ black hole and its charged generalization were calculated both analytically and numerically and compared with the corresponding QNMs of the vacuum TBH. It was found that there is a change in the slope of the QNMs as we decrease the value of the horizon radius below a critical value, and it has been argued that this change signals a phase transition of a vacuum topological black hole towards the MTZ black hole with scalar hair.

4 Stability analysis

To perform the stability analysis of the MTZ black hole it is more convenient to work in the Einstein frame (eqs. (2.19) and (2.20)). Henceforth, we shall work in units in which the radius of the boundary is $l = 1$.

The MTZ black hole metric can be written in the form

$$ds^2 = -\frac{f}{h^2} dt^2 + \frac{dr^2}{f} + r^2 d\sigma^2 \,, \tag{4.1}$$

where

$$\begin{aligned} f &= f_0(r) = \left[r^2 - \left(1 + \frac{r_0}{r}\right)^2 \right] \left(1 + \frac{r_0^2}{(r + 2r_0)(r + r_0)} \right)^2 \,, \\ h &= h_0(r) = \left(1 + \frac{r_0^2}{(r + 2r_0)(r + r_0)} \right) \frac{r + r_0}{\sqrt{r(r + 2r_0)}} \,, \end{aligned} \tag{4.2}$$

and the scalar field solution reads

$$\hat{\phi} = \phi_0(r) = \pm\sqrt{\frac{3}{4\pi G}}\tanh^{-1}\frac{r_0}{r+r_0}\ . \tag{4.3}$$

Since the potential (2.20) is an even function, the sign of ϕ_0 is arbitrary; we shall choose it so that the leading coefficient in the large r expansion is positive. Thus, for large r, we obtain

$$\hat{\phi}(r) = \frac{\alpha}{r} + \frac{c\alpha^2}{r^2} + \dots \tag{4.4}$$

where

$$\alpha = \alpha_0 = \sqrt{\frac{3}{4\pi G}}|r_0|\ , \qquad c = -\sqrt{\frac{4\pi G}{3}}\mathrm{sign}(r_0)\ . \tag{4.5}$$

Solutions to the Einstein equations with boundary conditions (4.5) have been found in the case of spherical horizons and shown to be unstable [21]. In that case, for $\alpha > 0$, it was shown that $c < 0$ always and the hairy black hole had positive mass. In our case, we also have $c < 0$ when the black hole has positive mass. However, we obtain $c > 0$ when the black hole has negative mass, which is never the case with spherical horizons.

We shall now show that in the former case the black hole is unstable (losing its hair to turn into a TBH) whereas in the latter, it is stable, as expected from thermodynamic considerations (see section 3).

To this end, we apply the perturbation [21]

$$f(r,t) = f_0(r) + f_1(r)e^{\mu t}, \quad h(r,t) = h_0(r) + h_1(r)e^{\mu t}, \quad \phi(r,t) = \phi_0(r) + \frac{\phi_1(r)}{r}e^{\mu t}\ . \tag{4.6}$$

with $\mu > 0$ for an instability to develop.

The field equations give a Schrödinger-like wave equation for the scalar perturbation,

$$-\frac{d^2\phi_1}{dr_*^2} + \mathcal{V}\phi_1 = -\mu^2\phi_1\,, \tag{4.7}$$

where we defined the tortoise coordinate

$$\frac{dr_*}{dr} = \frac{h_0}{f_0} \tag{4.8}$$

and the effective potential is given by

$$\mathcal{V} = \frac{f_0}{h_0^2}\left[-\frac{1}{2}\left(1 + r^2{\phi_0'}^2\right)\phi_0'^2 f_0 + \left(1 - r^2{\phi_0'}^2\right)\frac{f_0'}{r} + 2r\phi_0' V'(\phi_0) + V''(\phi_0)\right]\,, \tag{4.9}$$

as in the case of a spherical horizon [21].

Regularity of the scalar field at the horizon of the MTZ black hole ($r \to r_+$) requires the boundary conditions [21]

$$\phi_1 = 0\ , \qquad (r - r_+)\phi_1' = \kappa\mu\phi_1\ , \qquad \kappa > 0\ . \tag{4.10}$$

For a given $\mu > 0$, they uniquely determine the wavefunction.

JHEP07(2009)026

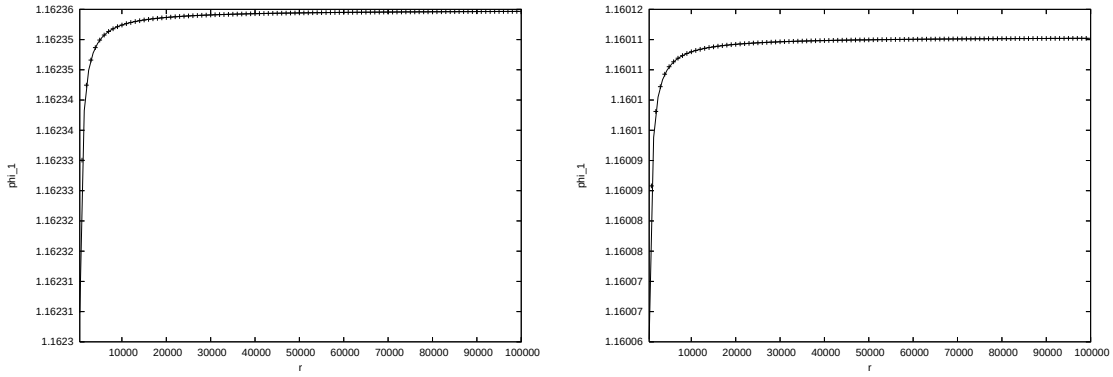

Figure 1. The perturbation ϕ_1 versus r for $\mu = 0.02$ and negative ($r_0 = -0.01$, left graph) or positive ($r_0 = -0.01$, right graph) value for r_0.

At the boundary, the wave equation is approximated by

$$-\frac{d^2\phi_1}{dr_*^2} + 5r_0^2\phi_1 = -\mu^2\phi_1\,, \tag{4.11}$$

with solutions

$$\phi_1 = e^{\pm E r_*}\ , \quad E = \sqrt{\mu^2 + 5r_0^2}\,, \tag{4.12}$$

where $r_* = -\frac{1}{r} + \dots$. Therefore, for large r,

$$\phi_1 = A + \frac{B}{r} + \dots \tag{4.13}$$

To match the boundary conditions (4.4) with c given by (4.5) and ϕ expanded as in (4.6), we need

$$\frac{B}{A} = -2r_0\ . \tag{4.14}$$

Since the wavefunction has already been determined by the boundary conditions at the horizon and therefore also the ratio B/A, this is a constraint on μ. If (4.14) has a solution, then the black hole is unstable. If it does not, then there is no instability of this type (however, one should be careful with non-perturbative instabilities, see [22]). In figure 1 we give sample results for both negative and positive values of r_0. If one fits these functions as in (4.13), it is obvious that $\frac{B}{A}$ will be negative in both cases. If r_0 is positive, equation (4.14) may have a solution for some value of μ, so there is an instability. On the contrary, if r_0 is negative, then $-2r_0 > 0$ and equation (4.14) has clearly no solution, so the black hole is stable.

5 The dual superconductor

Using the results of previous sections we will discuss the dual superconductor on the boundary of the exact supergravity solution. Recall that for $T < T_0$, a condensate forms ($\phi \neq 0$), the field equations have as a solution the MTZ black hole (2.14) and the scalar field is

JHEP07(2009)026

given by (2.15). For $T > T_0$, $\phi = 0$, no condensate forms and the field equations have as a solution the TBH of (2.8).

The metric on the boundary is given by (2.12) and its curvature is $-1/l$ (hyperbolic manifold). As in the previous section, we shall keep working in units in which the radius of the boundary is $l = 1$.

It should be noted that the mechanism of condensation of the scalar field here is different than the mechanism of condensation of the dual superconductor in the case of a black hole of flat horizon [7]. In the latter case the scalar field condenses because an Abelian-Higgs mechanism was in operation. In our case, the condensation of the scalar field has a geometrical origin and is due entirely to its coupling to gravity.

The energy of the superconductor which is dual to the hairy black hole solution is (eq. (2.21))

$$E_s(T) = M_{MTZ} = -\frac{\pi\sigma}{4G}\left(T_0^2 - T^2\right) , \tag{5.1}$$

which is negative for temperatures below the critical point T_0. However, notice that the negative contribution is entirely due to the Casimir energy. If we subtract the energy at $T = 0$, we obtain

$$E_s(T) - E_s(0) = \frac{\pi\sigma}{4G}\, T^2, \tag{5.2}$$

which is a positive quantity at all temperatures.

Moreover, the heat capacities in the normal and superconducting phases, dual to the TBH and MTZ solutions, respectively, are

$$C_n = T\frac{\partial S_{TBH}}{\partial T} \ , \quad C_s = T\frac{\partial S_{MTZ}}{\partial T} \ . \tag{5.3}$$

Using the explicit form of the entropy (eqs. (2.13) and (2.21)), near zero temperature we have

$$C_n \approx \frac{\pi\sigma}{3\sqrt{3}G}\, T \ , \quad C_s \approx \frac{\pi\sigma}{2G}\, T \, , \tag{5.4}$$

therefore both heat capacities vanish linearly with temperature as $T \to 0$. Such a power law dependence was also observed in the case of charged holographic superconductors in flat space [9], although the numerical value of the power could not be determined in that case. This departure from the typical behaviour of s-wave superconductors (exponential suppression of the heat capacity as $T \to 0$) may be due to the presence of a Goldstone mode [9].

To the exact gravity backgrounds we shall now apply an electromagnetic perturbation. In the case without a condensate (TBH) the wave equation for perturbing the vector potential reads [13]

$$f_{TBH}(f_{TBH}A')' + \left(\omega^2 - \frac{\xi^2 + 1/4}{r^2} f_{TBH}\right) A = 0 \, , \tag{5.5}$$

where A is an appropriately defined component of the vector potential.

The wavefunction of the lowest harmonic corresponds to the lowest eigenvalue in the compact hyperbolic space Σ (eq. (2.9)) given by

$$\xi^2 + \frac{1}{4} = 0 \ . \tag{5.6}$$

Defining the tortoise coordinate

$$r_* = -\int_r^\infty \frac{dr'}{f_{TBH}(r')}\,,$$

eq. (5.5) is solved to give (with arbitrary normalization)

$$A(r) = e^{-i\omega r_*} \tag{5.7}$$

which obeys the correct conditions at the horizon. For large r we have $r_* = -1/r + \mathcal{O}(r^{-3})$ therefore the vector potential at large radius behaves asymptotically as

$$A = A^{(0)} + \frac{A^{(1)}}{r} + \dots \tag{5.8}$$

According to the AdS/CFT correspondence, the dual source and the expectation value for the current in the same direction are given respectively by

$$A = A^{(0)}\,, \qquad \langle J\rangle = A^{(1)}\,. \tag{5.9}$$

Then the conductivity is

$$\sigma(\omega) = \frac{\langle J\rangle}{E} = -\frac{\langle J\rangle}{\dot{A}} = -\frac{\langle J\rangle}{i\omega A} = \frac{A^{(1)}}{i\omega A^{(0)}}\,. \tag{5.10}$$

We have $A^{(0)} = 1$, $A^{(1)} = i\omega$ and therefore the conductivity (5.10) reads

$$\sigma(\omega) = \frac{A^{(1)}}{i\omega A^{(0)}} = 1\,. \tag{5.11}$$

According to the discussion in the previous section, if the temperature is above the critical temperature $T_0 = \frac{1}{2\pi}$ (eq. (2.25) setting the radius $l = 1$), the most probable configuration is the vacuum TBH. Then relation (5.11) tell us that the boundary conducting theory is in the normal phase, as expected.

If the temperature is below the critical temperature, the vacuum TBH acquires hair and a condensate forms. In this case, (2.16) can be expanded as

$$\Psi = \frac{\Psi^{(1)}}{r} + \frac{\Psi^{(2)}}{r^2} + \dots\,, \tag{5.12}$$

where

$$\Psi^{(1)} = -\sqrt{\frac{3}{4\pi G}}\, r_0\,, \quad \Psi^{(2)} = \sqrt{\frac{3}{4\pi G}}\, r_0^2\,. \tag{5.13}$$

The two non-vanishing leading coefficients lead to condensates of two dual scalar operators $\mathcal{O}_i$ $(i = 1, 2)$, respectively,

$$\langle \mathcal{O}_i\rangle = \sqrt{2}\Psi^{(i)}\,, \quad i = 1, 2\,. \tag{5.14}$$

Unlike in the case of a flat horizon [7], the existence of two condensates does not imply an instability, as was shown in section 4.

JHEP07(2009)026

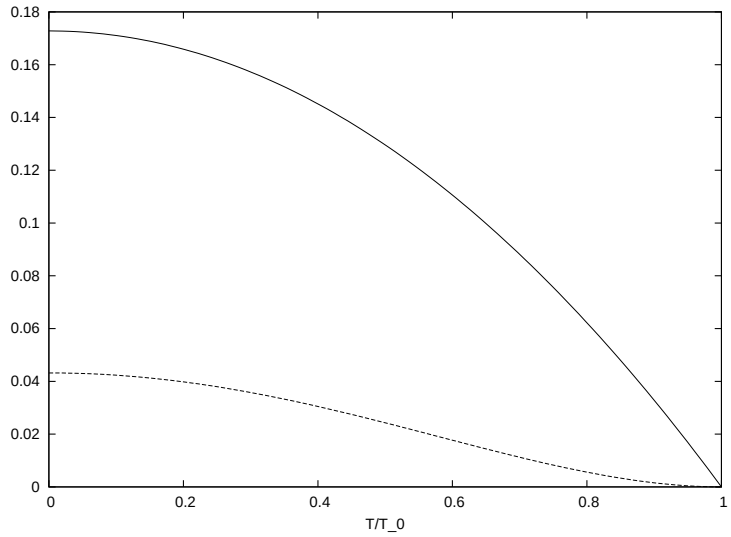

Figure 2. The condensates $\sqrt{G}\langle\mathcal{O}_1\rangle$ (upper curve) and $\sqrt{G}\langle\mathcal{O}_2\rangle$ (lower curve) as functions of T/T_0 (eq. (5.15)).

The two condensates (5.14) are, respectively,

$$\langle\mathcal{O}_1\rangle = \sqrt{\frac{3\pi^3}{2G}}\left(T_0^2 - T^2\right) , \quad \langle\mathcal{O}_2\rangle = \sqrt{\frac{3\pi^7}{2G}}\left(T_0^2 - T^2\right)^2 , \tag{5.15}$$

where we used (2.21) and (2.23) to express the condensates as functions of temperature. Near the critical temperature T_0 the condensates behave respectively as

$$\langle\mathcal{O}_1\rangle \simeq \sqrt{\frac{3}{8\pi G}}\left(1 - \frac{T}{T_0}\right) , \quad \langle\mathcal{O}_2\rangle \simeq \sqrt{\frac{3}{32\pi G}}\left(1 - \frac{T}{T_0}\right)^2 . \tag{5.16}$$

The two condensates are plotted as functions of temperature in figure 2. Observe that the condensates $\langle\mathcal{O}_1\rangle$, $\langle\mathcal{O}_2\rangle$ have a different temperature dependence than the corresponding operators in the dual superconductor of a black hole with flat horizon [7]. This behaviour of the condensates is reminiscent of materials containing impurities [23].

Applying the electromagnetic perturbations to this background, the wave equation for the vector potential reads

$$f_{MTZ}\left(f_{MTZ}A'\right)' + \left(\omega^2 - \frac{\xi^2 + 1/4}{r^2}f_{MTZ} - q^2\Psi^2 f_{MTZ}\right)A = 0 . \tag{5.17}$$

If we use the lowest angular eigenvalue (5.6), this simplifies to

$$f_{MTZ}\left(f_{MTZ}A'\right)' + \left(\omega^2 - q^2\Psi^2 f_{MTZ}\right)A = 0 . \tag{5.18}$$

eq. (5.18) can not be solved analytically in general. However, we can solve this equation for weak coupling q^2 using perturbation theory. Also, a numerical analysis of (5.18) will be presented in the next section. For $q = 0$ the solutions are $e^{\pm i\omega r_*}$ where

$$r_* = -\int_r^\infty \frac{dr'}{f_{MTZ}(r')} .$$

JHEP07(2009)026

The acceptable solution is $e^{-i\omega r_*}$. Using first-order perturbation theory, we obtain the solution

$$A = e^{-i\omega r_*} + \frac{q^2}{2i\omega} e^{i\omega r_*} \int_{r_+}^{r} dr' \Psi^2(r') e^{-2i\omega r_*} - \frac{q^2}{2i\omega} e^{-i\omega r_*} \int_{r_+}^{r} dr' \Psi^2(r') \ . \tag{5.19}$$

The lowest limit of the integration has been chosen at r_+ to ensure correct behaviour at the horizon. Expanding A in the large r limit (equation (5.8)), we get

$$A^{(0)} = A|_{r\to\infty} = 1 + \frac{q^2}{2i\omega} \int_{r_+}^{\infty} dr \Psi^2(r) \left[e^{-2i\omega r_*} - 1 \right] \ , \tag{5.20}$$

$$A^{(1)} = -r^2 \frac{dA}{dr}\bigg|_{r\to\infty} = i\omega - \frac{q^2}{2} \int_{r_+}^{\infty} dr \Psi^2(r) \left[e^{-2i\omega r_*} + 1 \right] \ . \tag{5.21}$$

Then, the conductivity to first-order in q^2 is

$$\sigma(\omega) = \frac{A^{(1)}}{i\omega A^{(0)}} = 1 - \frac{q^2}{i\omega} \int_{r_+}^{\infty} dr \Psi^2(r) e^{-2i\omega r_*} \ . \tag{5.22}$$

The superfluid density is the coefficient of the delta function of the real part of the conductivity

$$\Re[\sigma(\omega)] \sim \pi n_s \delta(\omega) \, , \tag{5.23}$$

which is also the coefficient of the pole in the imaginary part

$$\Im[\sigma(\omega)] \sim \frac{n_s}{\omega} \, , \quad \omega \to 0 \ . \tag{5.24}$$

Therefore using (5.22) we obtain for the superfluid density

$$n_s = q^2 \int_{r_+}^{\infty} dr \Psi^2(r) = \frac{3q^2}{4\pi G} \frac{r_0^2}{r_+ + r_0} \, , \tag{5.25}$$

or in terms of the temperature,

$$n_s(T) = \alpha \left(T_0 - T \right)^2 \ , \quad \alpha = \frac{3\pi q^2}{4G} \ . \tag{5.26}$$

Notice that near $T = 0$,

$$n_s(0) - n_s(T) \approx \frac{\alpha}{\pi} T \tag{5.27}$$

matching the low temperature behaviour of the heat capacity (5.4). Such power law behaviour was also observed in charged holographic superconductors in flat space [9]. Once again, we see an indication that a Goldstone mode is in play.

The normal, non-superconducting, component of the DC conductivity is given by

$$n_n = \lim_{\omega\to 0} \Re[\sigma(\omega)] \, . \tag{5.28}$$

We obtain

$$\ln n_n = 2q^2 \int_{r_+}^{\infty} dr \Psi^2(r) r_* \ . \tag{5.29}$$

JHEP07(2009)026

Integrating by parts, we obtain

$$\ln n_n = \frac{3q^2}{2\pi G} r_0^2 h(r_+)\,, \tag{5.30}$$

where

$$h(r_+) = -\frac{1}{r_0^2}\ln(r_+ + r_0) - \frac{1}{(r_+ + r_0)}\sum_{i=1}^{3}\frac{(r_+ - r_i)\ln(r_+ - r_i)}{f'_{MTZ}(r_i)(r_i + r_0)} \tag{5.31}$$

and r_i are the three horizons of MTZ black hole given in (2.23). At low temperatures we have $r_0 \to -\frac{1}{4}$ and the function $h(r_+)$ (5.31) is approximated by

$$h(r_+) \simeq -\frac{1}{(r_+ + r_0)}\frac{(r_+ - r_-)\ln(r_+ - r_-)}{f'_{MTZ}(r_-)(r_- + r_0)} \simeq 8\ln T\ . \tag{5.32}$$

Then the normal component of the DC conductivity (5.30) becomes

$$\ln n_n \simeq \frac{3q^2}{4\pi G}\ln T\ . \tag{5.33}$$

leading to the low temperature behaviour

$$n_n \sim T^\gamma\,, \quad \gamma = \frac{3q^2}{4\pi G}\ . \tag{5.34}$$

The approximation of the normal component of the DC conductivity (5.34) has a milder behaviour than the dual superconductor in the case of a black hole of flat horizon [7] in which n_n exhibits a clear gap behaviour. The behaviour we observe here of the boundary conducting theory can be found in materials with paramagnetic impurities [23] and in unconventional superconductors like the chiral p-wave superconductor [24].

These analytical results are supported by a numerical investigation of equation (5.18) which will be discussed in the next section.

6 Numerical results

In this section we discuss the numerical solution of the wave equation (5.18) in the interval $r \in [r_+, \infty)$ and compare it with the analytical results obtained above using perturbation theory. We shall be working in units in which the radius of the hyperbolic space is $l = 1$, so that, e.g., distances will be given in units of l and frequencies and temperatures will be in units of $1/l$.

The boundary condition at the horizon ($r = r_+$) is given by eq. (5.7) which implies

$$A'(r) = -\frac{i\omega}{f_{MTZ}(r)}A(r)\ . \tag{6.1}$$

Since, by definition, $f_{MTZ}(r_+) = 0$, we applied the boundary condition (6.1) at $r = r_+ + \epsilon$, where ϵ is a small positive quantity. In the following calculations the value $\epsilon = \frac{r_+}{10000}$ has been used. We integrated up to $r = R \equiv 5000 r_+$. We solved the wave equation for $r_+ \leq 1$ ($T \leq T_0$) since we know that in this temperature range the topological black hole acquires hair, while for $r_+ > 1$ the vacuum TBH is energetically favorable.

JHEP07(2009)026

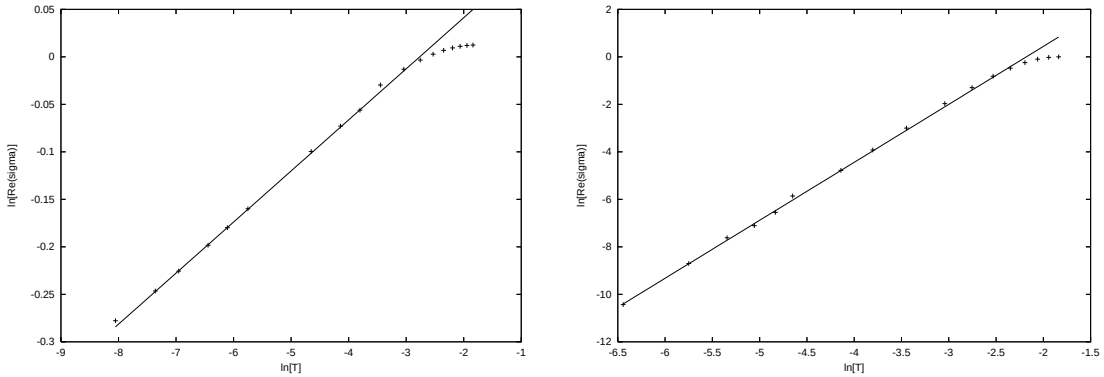

Figure 3. The logarithm of the normal fluid density as a function of the logarithm of the temperature for $q/\sqrt{G} = 0.5$ (left) and $q/\sqrt{G} = 5.0$ (right). The solid lines represent the fits $\ln n_n = 0.0538 \ln T + 0.149$ (left) and $\ln n_n = 2.45 \ln T + 5.3$ (right).

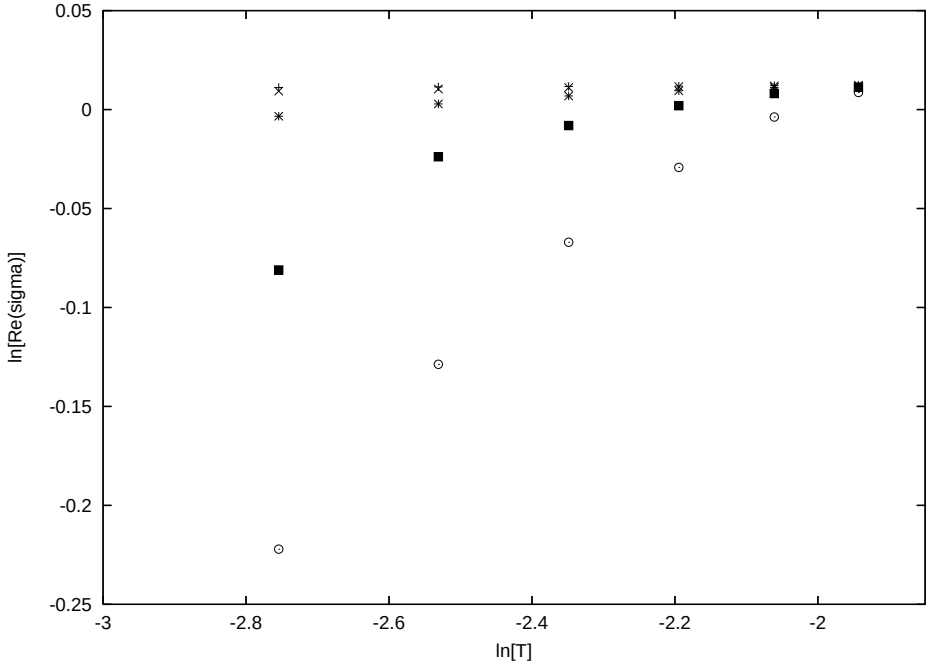

Figure 4. The logarithm of the real part of the conductivity as a function of the logarithm of the temperature for $q/\sqrt{G} = 0.1$ (crosses, the uppermost symbols), $0.2, 0.5, 1.0, 2.0$.

By curve fitting the solution of the wave equation, we calculated the coefficients $A^{(0)}$ and $A^{(1)}$ defined through (5.8). We then deduced the conductivity σ using (5.10). In the limit $\omega \to 0$, the conductivity yields the densities of the superfluid and normal components via (5.24) and (5.28), respectively. We chose $\omega = 0.001$ for our numerical calculations.

On the basis of the analytic results in section 5 we expect that at low temperature, the normal fluid density can be expanded as

$$\ln n_n = \gamma \ln T + \delta + \ldots \tag{6.2}$$

JHEP07(2009)026

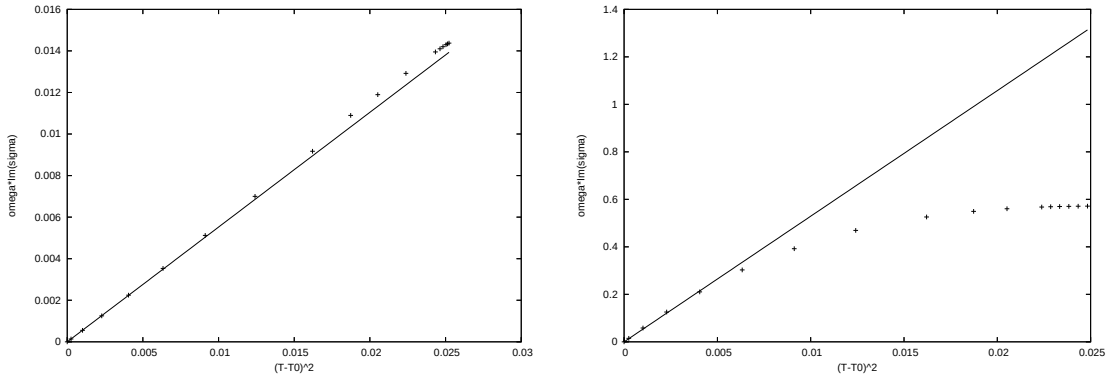

Figure 5. Superfluid density as a function of $(T - T_0)^2$ for $q/\sqrt{G} = 0.5$ (left) and $q/\sqrt{G} = 5.0$ (right). The solid lines represent the fits $n_s = 0.552(T - T_0)^2$ (left) and $n_s = 52.9(T - T_0)^2$ (right).

$q/\sqrt{G}$	$\gamma_{\text{numerical}}$	$\gamma_{\text{analytical}}$	$\alpha_{\text{numerical}}$	$\alpha_{\text{analytical}}$
0.1	0.0020	0.0024	0.0225	0.024
0.5	0.0538	0.0597	0.552	0.589
1.0	0.187	0.239	2.196	2.356
2.0	0.684	0.955	8.678	9.425
3.0	1.325	2.15	20.35	21.21
5.0	2.522	5.97	52.90	58.90

Table 1. Numerical *vs* analytical results for the normal and superfluid densities for various values of the charge. The numerical parameters are obtained through the fits (6.2) and (6.3), respectively. Their analytical counterparts are given by (5.34) and (5.26), respectively.

whereas near the critical temperature, the superfluid density is expanded as

$$n_s = \alpha(T - T_0)^2 + \dots \tag{6.3}$$

We therefore fit the data accordingly. The results for $\ln n_n$ at $q/\sqrt{G} = 0.5$ and $q/\sqrt{G} = 5.0$ are shown in figure 3. The fit (6.2) has taken into account only the points below $\ln T = -5$. This is why the data points at higher temperatures ($\ln T > -5$) lie below the fit.

Figure 4 contains data for various values of the charge q. We observe that the asymptotic slope of the curve as $T \to 0$ increases with the charge. Table 1 contains numerical values of the slope obtained through the fit (6.2) and compares them with their analytical counterparts (5.34).

We present our results for the superfluid density n_s *vs* temperature in figure 5 for $q/\sqrt{G} = 0.5, 5.0$. The fit has been done in the region of temperatures $(T - T_0)^2 < 0.005$, so it does not represent accurately the data at temperatures away from this region. Again, table 1 contains numerical values of the slope obtained through the fit (6.3) and compares them with their analytical counterparts (5.26). The agreement is better for n_s than for n_n.

At low temperatures, the superfluid density n_s approaches a constant. After subtract-

JHEP07(2009)026

$q/\sqrt{G}$	1	3	5
δ	1.025 ± 0.007	1.52 ± 0.03	1.78 ± 0.03

Table 2. The exponent δ characterizing the low temperature dependence of the superfluid density n_s (eq. (6.4)) for various values of the charge.

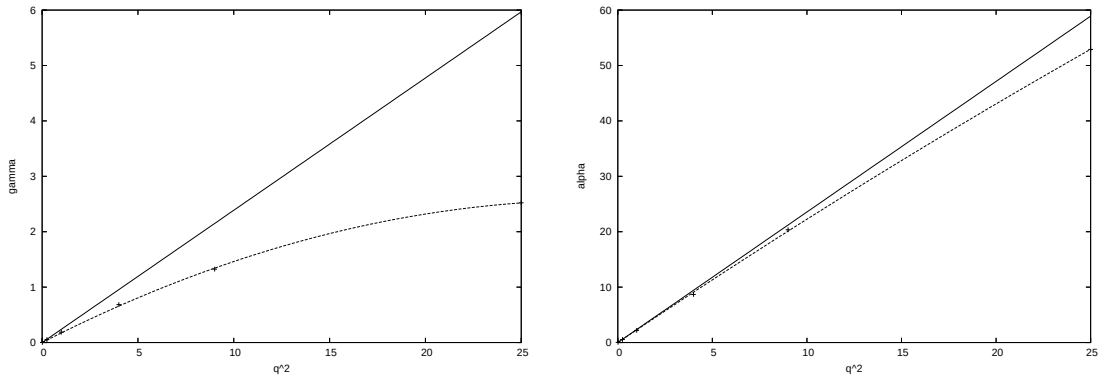

Figure 6. Numerical and analytical results for the normal (left) and superfluid (right) densities *vs* q^2. Numerical data are fitted by $0.176q^2 - 0.0030q^4$ (left) and $2.29q^2 - 0.007q^4$ (right).

ing this constant, we obtain the behaviour

$$n_s(0) - n_s(T) \sim T^\delta \tag{6.4}$$

where $\delta \approx 1$ for small charges q, in agreement with our earlier analytic result (5.27). Sample values of the exponent δ are shown in table 2. δ increases as q increases. Similar temperature dependence of n_s was observed in charged holographic superconductors in flat space [9] indicating the presence of a Goldstone mode.

The results of table 1 are depicted in figure 6. It is clear that the agreement between numerical and analytical results is quite satisfactory for the superfluid density, while serious discrepancies arise for the normal density as q increases.

We further analyzed the ω dependence of the transport coefficients. Figure 7 contains the real part of the conductivity *vs* ω for $q/\sqrt{G} = 2, 5$ and various values of the temperature. The lowest value of the temperature yields rather small values for this real part, while for larger temperatures the real part tends to the value 1, which is the outcome for the topological black hole. Comparing, one may see that the real part of the conductivity becomes smaller as we increase the charge q. Unfortunately, numerical instabilities also increase and we have not been able to produce reliable numerical results above $q/\sqrt{G} = 5$. In the cases we studied, it appears that the superconductor is *gapless*. However, a gap is likely to develop above a certain value of the charge q, as indicated by the trend in the graphs as q increases.

Finally, figure 8 contains the imaginary part of the conductivity *vs* ω for $q/\sqrt{G} = 2, 5$ and various values of the temperature. Some features are more clearly visible in the latter

JHEP07(2009)026

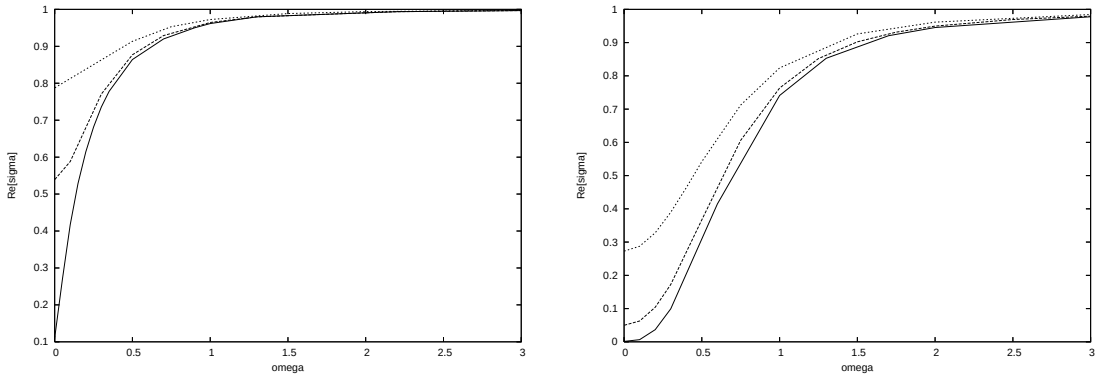

Figure 7. The real part of the conductivity *vs* ω for $q/\sqrt{G} = 2$ (left) and $q/\sqrt{G} = 5$ (right) and $T = 0.0032, 0.032, 0.064$. The lowest curve corresponds to the lowest temperature.

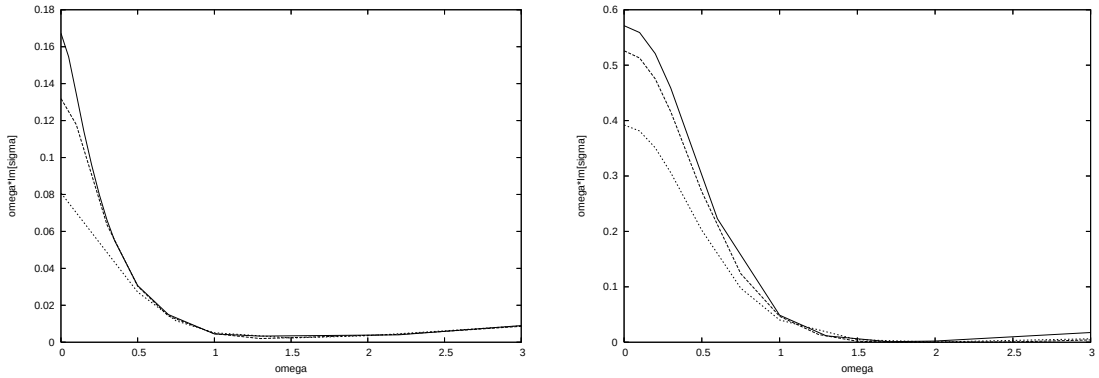

Figure 8. The imaginary part of the conductivity multiplied by ω *vs* ω for $q/\sqrt{G} = 2$ (left) and $q/\sqrt{G} = 5$ (right) and $T = 0.0032, 0.032, 0.064$. The uppermost curve corresponds to the lowest temperature.

case. The imaginary part is multiplied by ω to tame the pole at $\omega = 0$. The imaginary part seems to vanish at some frequency, which moves to the left as the temperature increases.

7 Conclusions

We presented a model of an exact gravity dual of a gapless superconductor in which a condensate forms as a result of the coupling of a charged scalar field to gravity. The charged scalar field responsible for the condensation is a solution of the field equations [11, 12] and below a critical temperature dresses up a vacuum black hole of a constant negative curvature horizon (TBH) with scalar hair. Perturbing the background Maxwell field and using the AdS/CFT correspondence, we determined the conductivity of the boundary theory and analysed the behaviour of the normal and superconducting fluid densities using both analytical and numerical techniques.

The condensation of the scalar field we considered had a purely geometrical origin being due entirely to its coupling to gravity. Hairy charged black hole solutions are also

JHEP07(2009)026

known to exist in the case of a *real* scalar field [12]. It would be interesting to extend these solutions to the case of a *complex* (charged) scalar field ϕ and analyse the entire range of parameters labeling the solutions, including the charges of the black hole and the scalar field. This should yield an interesting landscape consisting of chargeless as well as charged superconductors, as in the flat case [7, 9]. Work in this direction is in progress.

Acknowledgments

Work supported by the NTUA research program PEVE07. G. S. was supported in part by the US Department of Energy under grant DE-FG05-91ER40627.

References

[1] J.M. Maldacena, *The large-N limit of superconformal field theories and supergravity*, *Adv. Theor. Math. Phys.* **2** (1998) 231 [*Int. J. Theor. Phys.* **38** (1999) 1113] [hep-th/9711200] [SPIRES].

[2] D. Mateos, *String theory and quantum chromodynamics*, *Class. Quant. Grav.* **24** (2007) S713 [arXiv:0709.1523] [SPIRES].

[3] S.A. Hartnoll and P. Kovtun, *Hall conductivity from dyonic black holes*, *Phys. Rev.* **D 76** (2007) 066001 [arXiv:0704.1160] [SPIRES].

[4] S.A. Hartnoll, P.K. Kovtun, M. Muller and S. Sachdev, *Theory of the Nernst effect near quantum phase transitions in condensed matter and in dyonic black holes*, *Phys. Rev.* **B 76** (2007) 144502 [arXiv:0706.3215] [SPIRES].

[5] S.A. Hartnoll and C.P. Herzog, *Ohm's Law at strong coupling: s duality and the cyclotron resonance*, *Phys. Rev.* **D 76** (2007) 106012 [arXiv:0706.3228] [SPIRES].

[6] S.A. Hartnoll and C.P. Herzog, *Impure AdS/CFT*, *Phys. Rev.* **D 77** (2008) 106009 [arXiv:0801.1693] [SPIRES].

[7] S.A. Hartnoll, C.P. Herzog and G.T. Horowitz, *Building a holographic superconductor*, *Phys. Rev. Lett.* **101** (2008) 031601 [arXiv:0803.3295] [SPIRES].

[8] S.S. Gubser, *Breaking an Abelian gauge symmetry near a black hole horizon*, *Phys. Rev.* **D 78** (2008) 065034 [arXiv:0801.2977] [SPIRES].

[9] S.A. Hartnoll, C.P. Herzog and G.T. Horowitz, *Holographic superconductors*, *JHEP* **12** (2008) 015 [arXiv:0810.1563] [SPIRES].

[10] M. Ammon, J. Erdmenger, M. Kaminski and P. Kerner, *Superconductivity from gauge/gravity duality with flavor*, arXiv:0810.2316 [SPIRES].

[11] C. Martinez, R. Troncoso and J. Zanelli, *Exact black hole solution with a minimally coupled scalar field*, *Phys. Rev.* **D 70** (2004) 084035 [hep-th/0406111] [SPIRES].

[12] C. Martinez, J.P. Staforelli and R. Troncoso, *Charged topological black hole with a conformally coupled scalar field*, *Phys. Rev.* **D 74** (2006) 044028 [hep-th/0512022] [SPIRES];
C. Martinez and R. Troncoso, *Electrically charged black hole with scalar hair*, *Phys. Rev.* **D 74** (2006) 064007 [hep-th/0606130] [SPIRES].

JHEP07(2009)026

[13] G. Koutsoumbas, S. Musiri, E. Papantonopoulos and G. Siopsis, *Quasi-normal modes of electromagnetic perturbations of four-dimensional topological black holes with scalar hair*, *JHEP* **10** (2006) 006 [hep-th/0606096] [SPIRES].

[14] I. Papadimitriou, *Non-supersymmetric membrane flows from fake supergravity and multi-trace deformations*, *JHEP* **02** (2007) 008 [hep-th/0606038] [SPIRES].

[15] R.B. Mann, *Pair production of topological anti-de Sitter black holes*, *Class. Quant. Grav.* **14** (1997) L109 [gr-qc/9607071] [SPIRES]; *Charged topological black hole pair creation*, *Nucl. Phys.* **B 516** (1998) 357 [hep-th/9705223] [SPIRES];
D.R. Brill, J. Louko and P. Peldan, *Thermodynamics of (3+1)-dimensional black holes with toroidal or higher genus horizons*, *Phys. Rev.* **D 56** (1997) 3600 [gr-qc/9705012] [SPIRES];
D. Birmingham, *Topological black holes in anti-de Sitter space*, *Class. Quant. Grav.* **16** (1999) 1197 [hep-th/9808032] [SPIRES].

[16] L. Vanzo, *Black holes with unusual topology*, *Phys. Rev.* **D 56** (1997) 6475 [gr-qc/9705004] [SPIRES].

[17] N.L. Balazs and A. Voros, *Chaos on the pseudosphere*, *Phys. Rept.* **143** (1986) 109 [SPIRES].

[18] P. Breitenlohner and D.Z. Freedman, *Stability in gauged extended supergravity*, *Ann. Phys.* **144** (1982) 249 [SPIRES].

[19] L. Mezincescu and P.K. Townsend, *Stability at a local maximum in higher dimensional anti-de Sitter space and applications to supergravity*, *Ann. Phys.* **160** (1985) 406 [SPIRES].

[20] G. Koutsoumbas, E. Papantonopoulos and G. Siopsis, *Stability analysis of hairy black holes in AdS space*, in preparation.

[21] T. Hertog and K. Maeda, *Stability and thermodynamics of AdS black holes with scalar hair*, *Phys. Rev.* **D 71** (2005) 024001 [hep-th/0409314] [SPIRES].

[22] E. Witten and S.-T. Yau, *Connectedness of the boundary in the AdS/CFT correspondence*, *Adv. Theor. Math. Phys.* **3** (1999) 1635 [hep-th/9910245] [SPIRES].

[23] S. Skalski, O. Betbeder-Matibet, and P. R. Weiss, *Properties of superconducting alloys containing paramagnetic impurities*, *Phys. Rev.* **136** (1964) A1500.

[24] M.M. Roberts and S.A. Hartnoll, *Pseudogap and time reversal breaking in a holographic superconductor*, *JHEP* **08** (2008) 035 [arXiv:0805.3898] [SPIRES].

JHEP07(2009)026